Nanoscale Advances

ROYAL SOCIETY OF CHEMISTRY

PAPER

View Article Online
View Journal | View Issue



Cite this: *Nanoscale Adv.*, 2025, **7**, 3867

# Synergistic effect of gold nanorods coated with type I collagen and LED irradiation on wound healing in human skin fibroblast cells

Sasiprapa Poomrattanangoon[ab] and Dakrong Pissuwan *[ab]

Delayed wound healing poses a significant risk to human health, especially when wounds are infected by pathogens. Therefore, the development of effective methods for accelerating wound healing is important. This study investigated the synergistic effect of gold nanorods (GNRs) coated with type I collagen (GNRs@C) combined with light-emitting diode (LED) irradiation on wound healing in scratched human skin fibroblast (HSF) cells. Scratched HSF cells were treated with 3 μg $mL^{-1}$ GNRs@C, followed by LED irradiation. This combined treatment significantly enhanced cell proliferation, increasing from the control cell base line (scratched HSF cells without any treatment) to 104.08 ± 2.96% and 107.82 ± 3.25% after 24 and 48 h of incubation, respectively. GNRs@C demonstrated superior cellular uptake compared to uncoated GNRs. Notably, complete closure of scratched HSF cells was observed in scratched HSF cells treated with GNRs@C with LED irradiation and then incubated for 40 h. Additionally, the treatment significantly reduced interleukin-6 (IL-6) and tumor necrosis factor-alpha (TNF-α) levels, while upregulating key growth factors, including vascular endothelial growth factor (VEGF) and basic fibroblast growth factor (bFGF). These findings demonstrate the wound healing potential of GNRs@C combined with LED irradiation.

Received 27th December 2024
Accepted 9th May 2025

DOI: 10.1039/d4na01072h

rsc.li/nanoscale-advances



## Introduction

Gold nanorods (GNRs) are rod-shaped gold nanoparticles that exhibit excellent optical properties owing to their localized surface plasmon resonance effect. This effect refers to the collective oscillation of electrons at the surface of GNRs excited by light, which can convert light to heat energy.[1] Their surfaces can be easily modified to enhance their interactions with biological systems[2] and reduce the toxicity arising from cetyltrimethylammonium bromide (CTAB). For example, Salah *et al.*[3] demonstrated that surface-modified GNRs can be successfully used in bioimaging and photoacoustic imaging. Wan *et al.*[4] modified the surface of GNRs with polyelectrolytes resulting in decreased toxicity to human embryonic kidney 293T (HEK293T) cells, human fetal hepatocyte (L02) cells, and human foreskin fibroblasts (HFF) cells. These studies showed that biocompatible GNRs have great potential for biological applications. A wound is skin or tissue damaged by physical, chemical, or medical factors.[5] The process of wound healing is important because it prevents negative effects such as inflammation, infection, and other diseases that may arise due to a delayed healing process.[6] Therefore, the development of techniques that stimulate wound healing can reduce the problems associated with wound healing.[7]

GNRs have also been reported to stimulate wound healing. For instance, Mahmoud *et al.*[8] reported that the surfaces of GNRs modified with polyacrylic acid (PAA), polyethylene glycol (PEG), and amine ($NH_2$) promoted the migration of fibroblast cells after 24 h of incubation with surface-modified GNRs. Additionally, Soliman *et al.*[9] demonstrated that GNRs in a hydroxypropyl methylcellulose (HPMC) hydrogel promoted wound healing in diabetic Male Wistar rats and provided antibacterial activity against *E. coli*, *S. aureus*, and *C. albicans*. This antibacterial effect could occur through the surface coating of the GNRs. An interaction between GNRs and bacterial cell walls that causes cell content leakage and bacterial death has also been reported.[10,11]

Currently, low-level laser therapy (LLLT), which uses low intensity light through lasers or light-emitting diodes (LEDs), is attractive for wound healing,[12] pain relief,[13] and inflammation reduction.[14] Many studies have demonstrated the biological effects of LLLT on wound healing. The photoreceptor molecule of the mitochondria, cytochrome C oxidase (CCO), can absorb red/infrared light. This absorption increases the levels of nitric oxide (NO), reactive oxygen species (ROS), and adenosine triphosphate (ATP).[15] The production of ATP can lead to an increase in pH, cyclic adenosine monophosphate, $Ca^{2+}$, and $K^{+}$,[16] which are critical for regulating gene expression related to

[a]*Materials Science and Engineering Program, Faculty of Science, Mahidol University, Bangkok 10400, Thailand*

[b]*Nanobiotechnology and Nanobiomaterials Research Laboratory, School of Materials Science and Innovation, Faculty of Science, Mahidol University, Bangkok 10400, Thailand. E-mail: dakrong.pis@mahidol.ac.th*

cell proliferation.[17] Furthermore, increased levels of ATP, NO, and ROS can promote the activation of intracellular signalling pathways and transcription factors, including nuclear factor kB (NF-kB) and activator protein-1 (AP-1).[18] These signalling pathways and factors are related to cell migration, proliferation, apoptosis, and adhesion.[17] Owing to their optical properties, GNRs can cooperate with LLLT to enhance wound healing.[19] As mentioned earlier, LEDs are among the light sources used in LLLT. They have many advantages such as low cost, long lifetime, user safety, and low energy usage.[19] For example, Poorani *et al.*[20] demonstrated that GNRs combined with LEDs were used to treat Vero cells and heat energy was then generated from the GNRs. Type I collagen is a fibril-forming collagen located in connective tissues such as the skin, bone, and ligament. This type of collagen provides good tensile strength and can act as a biological scaffold to support cells.[21] Type I collagen can bind to inflammatory cytokines such as interleukin-6 (IL-6) and interleukin-8 (IL-8) resulting in the formation of a wound milieu that can enhance wound healing.[22]

Given the benefits of LEDs, GNRs, and type I collagen, we were interested in investigating the effect of GNRs in combination with LED irradiation and type I collagen on wound-healing enhancement. The surface of the GNRs was modified by applying poly(sodium 4-styrenesulfonate) (PSS) and type I collagen, leading to the formation of GNRs@C. Scratched human skin fibroblast (HSF) cells were used as an *in vitro* wound model. The scratched HSF cells were treated with GNRs@C in combination with LED irradiation. It is important to note that the GNRs@C used in our study were in a colloidal form and were not incorporated into a biomaterial scaffold. Therefore, our investigation focused on the effects of GNRs@C, with or without LED exposure, on parameters relevant to wound healing activity, including cell toxicity, cell proliferation, cell migration, cellular uptake, inflammatory cytokines, and the expression of growth factors.

# Experimental section

## Materials

Gold(III) chloride solution, sodium borohydride ($NaBH_4$), silver nitrate ($AgNO_3$), and PSS were purchased from Sigma-Aldrich (St. Louis, MO, USA). Cetyltrimethylammonium bromide (CTAB) was purchased from HIMEDIA (Mumbai, India). Rat tail collagen at a concentration of 2 mg $mL^{-1}$ was purchased from Serva (Heidelberg, Germany). High glucose Dulbecco's modified Eagle's medium (DMEM), fetal bovine serum (FBS), and penicillin/streptomycin were purchased from HIMEDIA (Mumbai, India). The CellTiter-Glo luminescent cell viability assay and CellTiter 96 AQueous One Solution cell proliferation assay were purchased from Promega (Madison, WI, USA). Phosphate-buffered saline (PBS) solution containing $Ca^{2+}$ and $Mg^{2+}$ (100×) was purchased from NacalaiTesque (Kyoto, Japan). An Araldite 502 epoxy resin kit was purchased from EMS (Hatfield, PA, USA). Hydrogen peroxide ($H_2O_2$) was purchased from The Government Pharmaceutical Organization (Bangkok, Thailand). The enzyme-linked immunosorbent assay MAX Deluxe set of human IL-6, basic fibroblast growth factor (bFGF), and tumor necrosis factor-alpha (TNF-α) were purchased from BioLegend (San Diego, CA, USA). The human vascular endothelial growth factor (VEGF) ELISA kit was purchased from Abcam (Cambridge, MA, USA).

## Synthesis of GNRs and GNRs@C

To synthesize GNRs, the seed solution was prepared by adding 2 μL of 2% $HAuCl_4$ to 450 μL of 0.1 M CTAB. Following this, the cold $NaBH_4$ (0.1 M, 1.2 μL) was added. Next, the solution was mixed immediately at a high speed and then incubated at room temperature for 2 h. The growth solution was prepared by adding 50 μL of 0.1 M $AgNO_3$ to 750 μL of 24.28 mM $HAuCl_4$. This mixture was later mixed with 50 mL of 0.1 M CTAB, 750 μL of 1 M NaOH, and 137.5 μL of 6% $H_2O_2$, respectively. The whole mixture was then mixed for 1 min using a high-speed mixer. Next, the prepared seed solution (150 μL) was added to the growth solution and then briefly mixed again with a high-speed mixer. Finally, the mixture of the seed and growth solution was incubated at room temperature for 1.5 h to form GNRs.

The surface modification of GNRs with PSS was performed by centrifuging GNRs at 9391×*g* for 10 min twice to remove the extra CTAB. Then, 300 μL of 2 mg $mL^{-1}$ PSS (dissolved in 0.5 mM NaCl) was added to 600 μL GNRs. Subsequently, the mixture was shaken for 30 min using a shaker. Thereafter, the mixed solution was centrifuged twice at 9391×*g* for 10 min to remove the free PSS. The pellet of GNRs@PSS was collected for conjugation with type I collagen. Conjugation was performed by adjusting the optical density (O.D.) of GNRs@PSS at a wavelength of 644 nm to 1.0. Thereafter, a mixture of GNRs@PSS and 2 mg $mL^{-1}$ type I collagen at a ratio of 1 : 1 was prepared. The mixture was shaken for 15 min and then centrifuged at 9391×*g* for 10 min. The pellet of GNRs@PSS conjugated with type I collagen (GNRs@C) was dispersed in Milli-Q water, and used for further experiments.

## Characterization of GNRs

The light absorption of the GNRs was characterized using a UV-vis spectrophotometer (UV-2550, Shimadzu, Kyoto, Japan). The morphology and average size of the GNRs were investigated using transmission electron microscopy (TEM, JEOL, Tokyo, Japan). Zeta potential was measured using dynamic light scattering (ZetaSizer, Malvern Panalytical, Malvern, UK).

Fourier transform infrared (FT-IR) spectroscopy was also used to investigate the surface modification of GNRs with type I collagen. The samples were prepared by centrifuging GNRs@PSS and GNRs@C (1 mL each) at 9391×*g* for 10 min at room temperature. After centrifugation, the pellet was placed on a glass slide and dried in a silica gel box. The dropping and drying of samples were repeated 10 times to concentrate the concentration of GNRs@PSS or GNRs@C. The type I collagen sample was also prepared using the same procedure. Finally, the prepared samples were measured their infrared (IR) spectra using FT-IR with attenuated total reflection (ATR) mode at scan wavelengths 400 to 4000 $cm^{-1}$ with a spectral

resolution of 4 $cm^{-1}$ and the number of scans was 16 scans per sample (Thermo Scientific™, Waltham, MA, USA).

### Cell culture

HSF cells were purchased from the National Institute of Biomedical Innovation, Health, and Nutrition (NIBIOHN). The cells were cultured in DMEM medium (high glucose) supplemented with 10% FBS and 1% penicillin/streptomycin. The HSF cells were incubated in a 5% $CO_2$ incubator at 37 °C.

### Cell viability

HSF cells ($1 \times 10^4$ cells per well) were seeded in a 96-well plate and incubated at 37 °C in an incubator supplied with 5% $CO_2$ for 24 h. HSF cells were then treated with different concentrations of GNRs, GNRs@PSS, and GNRs@C (3, 5, 10, 15, and 25 μg $mL^{-1}$) for 5 h. After that, the treated HSF cells were exposed to LEDs (with an output power of ∼2.3 mW, a wavelength of ∼638 nm, and a spot size of ∼0.65 cm) for 5 min and incubated for another 24 h. An energy density was 2.08 J $cm^{-2}$. HSF cells treated with prepared nanoparticles without LED irradiation were incubated for 24 h. After incubation, cell viability was measured using the CellTiter-Glo luminescent cell viability assay (Promega, Madison, WI, USA). Luminescent signals were measured using a microplate reader (TECAN Spark 10 M, Männedorf, Switzerland). HSF cells without any treatment were used as control cells.

Subsequent experiments involving LED irradiation were conducted using identical output power, exposure time, and spot size as those used in the cell viability experiment.

### Cell proliferation

HSF cells at a concentration of $1 \times 10^4$ cells per well were added to a 96-well plate and incubated for 24 h. HSF cells were then treated with GNRs, GNRs@PSS, and GNRs@C at the same concentrations as those used in the cell viability test. The treatment procedure was the same as the cell viability test; however, cell proliferation was measured using the CellTiter 96 AQueous One Solution cell proliferation assay (Promega, Madison, WI, USA). After the reaction, the absorbance of the samples was measured at 490 nm using a microplate reader (TECAN Spark 10 M, Männedorf, Switzerland).

### *In vitro* wound scratch assay

HSF cells were seeded in a 96-well plate ($1 \times 10^4$ cells per well) and incubated for 24 h. The cells were then scratched using a 200 μL sterile tip and washed twice with PBS containing $Ca^{2+}$ and $Mg^{2+}$. After washing, the scratched HSF cells were treated with 3 μg $mL^{-1}$ of GNRs, GNRs@PSS, or GNRs@C in DMEM medium (high glucose) supplemented with 5% FBS and 1% penicillin/streptomycin for 5 h. After that, the cells were exposed to LED for 5 min and the gap was measured at 0 h. The gap of treated scratched HSF cells without LED irradiation was also measured at 0 h and then incubated for 24 h. Untreated scratched HSF cells were used as control cells. Thereafter, post-wounding gaps were measured after 16, 24, 40, and 48 h of incubation. The area of the gap was measured using ImageJ software and the percentage of wound closure were calculated.

$$\frac{(A_0 - A_T)}{A_0} \times 100$$

In this equation, $A_0$ represents the initial gap area at 0 h and $A_T$ is the gap area measured at a specific time point (h).[23]

### Cellular uptake

To investigate the cellular uptake of GNRs, HSF cells were seeded in a 96-well plate ($1 \times 10^4$ cells per well) and incubated for 24 h. Then, the cells were scratched using a 200 μL sterile tip and washed twice with PBS containing $Ca^{2+}$ and $Mg^{2+}$. After washing, the scratched HSF cells were treated with 3 μg $mL^{-1}$ GNRs@PSS or GNRs@C in DMEM medium (high glucose) supplemented with 5% FBS and 1% penicillin/streptomycin for 5 h. The cells were then exposed to LED irradiation and incubated for 24 and 48 h. Following incubation, HSF cells treated with GNRs@PSS or GNRs@C were added with 100 μL of cell lysis buffer (10% tween-20 in PBS without $Ca^{2+}$ and $Mg^{2+}$) to break the cell membrane. Thereafter, cells were digested in a digestion buffer (3 mL of 65% HCl and 1 mL of 6% $H_2O_2$) in a dark fume hood overnight. After incubation with the digestion buffer, 3 mL of aqua regia was added to the cell samples and incubated for another 2 h. Following this step, the cell samples were adjusted to a volume of 100 mL with Milli-Q water. Standard gold chloride solutions were prepared at concentrations of 0, 2.5, 5, 10, 20, 25, and 50 μg $L^{-1}$. Next, 5% aqua regia was added to each concentration. The gold content of the cell samples was measured using inductively coupled plasma mass spectrometry (ICP-MS) (Agilent Technologies, Santa Clara, CA, USA).[24]

### Detection of Ki67 expression

Since Ki67 is a cellular marker widely used to confirm cell proliferation,[25] the expression of Ki67 protein in HSF cells was also investigated using immunocytochemistry technique. First, HSF cells were seeded at $1 \times 10^4$ cells in a 35 mm clear coverglass-bottom Petri dish and incubated for 24 h. Next, HSF cells were scratched with a 200 μL sterile pipette tip and washed twice with PBS containing $Ca^{2+}$ and $Mg^{2+}$. Then, HSF cells were treated with 3 μg $mL^{-1}$ of GNRs@PSS or GNRs@C and cultured in DMEM medium with high glucose supplemented with 5% FBS and 1% penicillin/streptomycin for 5 h. After treatment, the HSF cells were exposed to LED irradiation for 5 min and incubated for 48 h. Thereafter, the HSF cells were fixed with 4% paraformaldehyde in PBS for 15 min at room temperature and washed twice with PBS containing $Ca^{2+}$ and $Mg^{2+}$. A non-specific binding was blocked using blocking buffer (0.3% Triton-X100) in PBS supplemented with 1% bovine serum albumin (BSA) for 40 min. Thereafter, the cell samples were gently washed twice with PBS containing $Ca^{2+}$ and $Mg^{2+}$. After washing, the cell samples were treated with a primary antibody (anti-Ki-67 antibody; clone Ki-S5 (a high quality mouse monoclonal antibody for the detection of Ki-67); Merck-Millipore, Darmstadt, Germany).

The anti-Ki-67 antibody was diluted with 1% BSA at a 1 : 400 dilution. The cells were incubated with the prepared anti-Ki-67 antibody for 1 h at room temperature. Following this, the cell samples were washed twice with PBS containing $Ca^{2+}$ and $Mg^{2+}$, and then stained with goat anti-mouse IgG (H + L) cross-adsorbed secondary antibody, Alexa Fluor™ 488 (dilution 1 : 600, ThermoFisher Scientific, Waltham, MA, USA). The diluent was 1% BSA. The stained cells were incubated for 1 h at room temperature and then washed twice with PBS containing $Ca^{2+}$ and $Mg^{2+}$. Next, the cell samples were mounted using a ProLong™ gold antifade mountant with 4′,6-diamidino-2-phenylindole, dihydrochloride (DAPI) reagent (ThermoFisher Scientific, Waltham, MA, USA) by dropping this reagent and placing a coverslip onto the cell samples. Finally, the cell samples were incubated at room temperature in the dark for 24 h and cell samples were then imaged using a fluorescent microscope (Olympus, Tokyo, Japan). Fluorescence intensities were quantified using the ImageJ software.

### ELISA

The supernatants of the scratched SF cells treated with GNRs@PSS or GNRs@C were collected to determine the production of inflammatory cytokines (IL-6 and TNF-α). The supernatants of the control cells were also collected. ELISA kits from BioLegend (San Diego, CA, USA) were used and measurements were performed according to the manufacturer's instructions. Angiogenic growth factors, vascular endothelial growth factor (VEGF), and basic fibroblast growth factor (bFGF), were also measured using ELISA kits (Abcam, Cambridge, USA). The analysis was performed according to the manufacturer's instructions. Absorbances were measured at 450 nm using a microplate reader (TECAN Spark 10 M, Männedorf, Switzerland).

### Statistical analysis

Experimental data of this study are shown as mean ± standard error of the mean. Statistical analyses were performed using GraphPad Prism software version 8. Analysis of variance (ANOVA) and Tukey–Kramer tests were performed to determine statistical significance at $P \leq 0.05$. Untreated control cells were used in all cell-related experiments for comparison.

## Results and discussion

### Characterization of GNRs with different surface modifications

The light absorption of the GNRs with different surface modifications was measured. As shown in Fig. 1, two typical plasmon resonant peaks of GNRs were detected. The first peak is from the transverse surface plasmon resonance (TSPR) mode and the second peak corresponds to the longitudinal surface plasmon resonance (LSPR) mode.[2,26] GNRs@PSS exhibited TSPR and LSPR peaks at 543 and 644 nm, respectively. These peaks were similar to those of the original surface GNRs at 542 and 643 nm for TSPR and LSPR, respectively (Fig. 1(a)). The results obtained in this study were comparable to those of a previous investigation, which demonstrated that modifying the surface of GNRs with PSS did not produce a significant shift in the TSPR and LSPR peaks.[27] When GNRs@PSS were coated with type I collagen (GNRs@C), the TSPR and LSPR peaks of GNRs@C exhibited a red shift from 543 to 551 nm and 644 to 658 nm, respectively. These red shifts were attributed to changes in the refractive index of the surrounding medium caused by the coating of GNRs@PSS with type I collagen.[28,29] Therefore, our results confirm that the surface of GNRs@PSS was successfully coated with type I collagen.

The morphologies of GNRs, GNRs@PSS, and GNRs@C are shown in Fig. 2(a–c). According to the TEM images, the average sizes of GNRs, GNRs@PSS, and GNRs@C were measured. The average widths of GNRs, GNRs@PSS, and GNRs@C were 12.01 ± 0.23, 14.60 ± 0.41, and 13.92 ± 0.43 nm, respectively. The average lengths of GNRs, GNRs@PSS, and GNRs@C were 26.06 ± 0.35, 29.64 ± 0.68, and 28.00 ± 0.47 nm, respectively. The zeta potential of original GNRs was 39.53 ± 0.50 mV and decreased to −43.43 ± 0.75 mV after modifying with PSS, GNRs@PSS. The decrease in zeta potential was due to anionic groups of PSS.[30]

When GNRs@PSS were modified with type I collagen, the zeta potential of GNRs@C appeared to have a positive value (20.70 ± 0.55 mV) because of the amino group from collagen[31] (Fig. 2(d)). This result indicates the adsorption of collagen on the surface of GNRs@PSS. Yu *et al.*[32] also reported that the

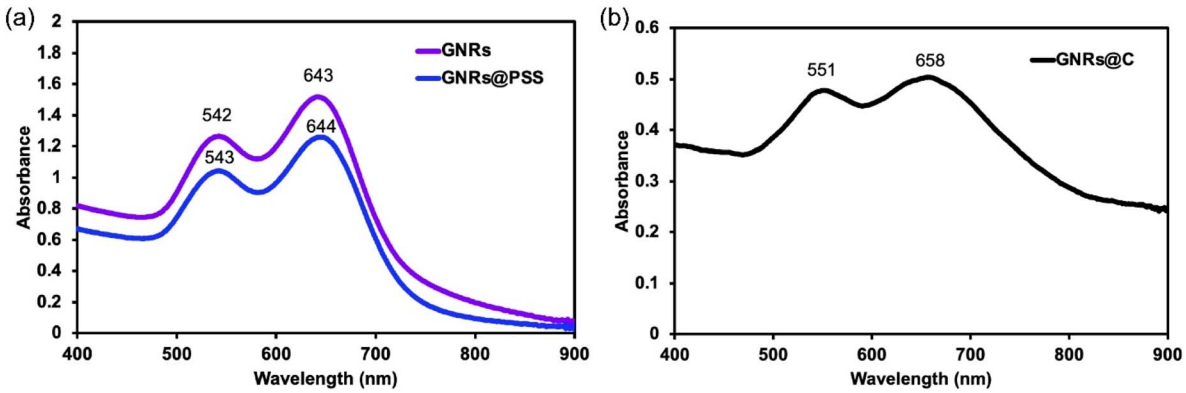


Fig. 1 Light absorption spectra of (a) GNRs and GNRs@PSS (b) GNRs@C.

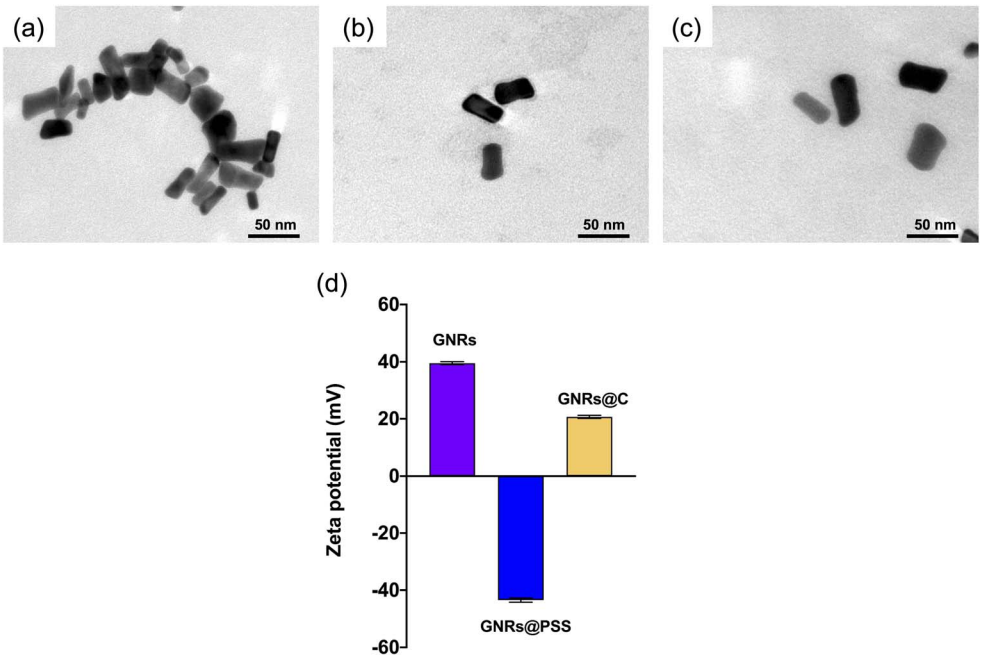


Fig. 2 TEM images of (a) GNRs, (b) GNRs@PSS and (c) GNRs@C and (d) zeta potentials of GNRs, GNRs@PSS, and GNRs@C.

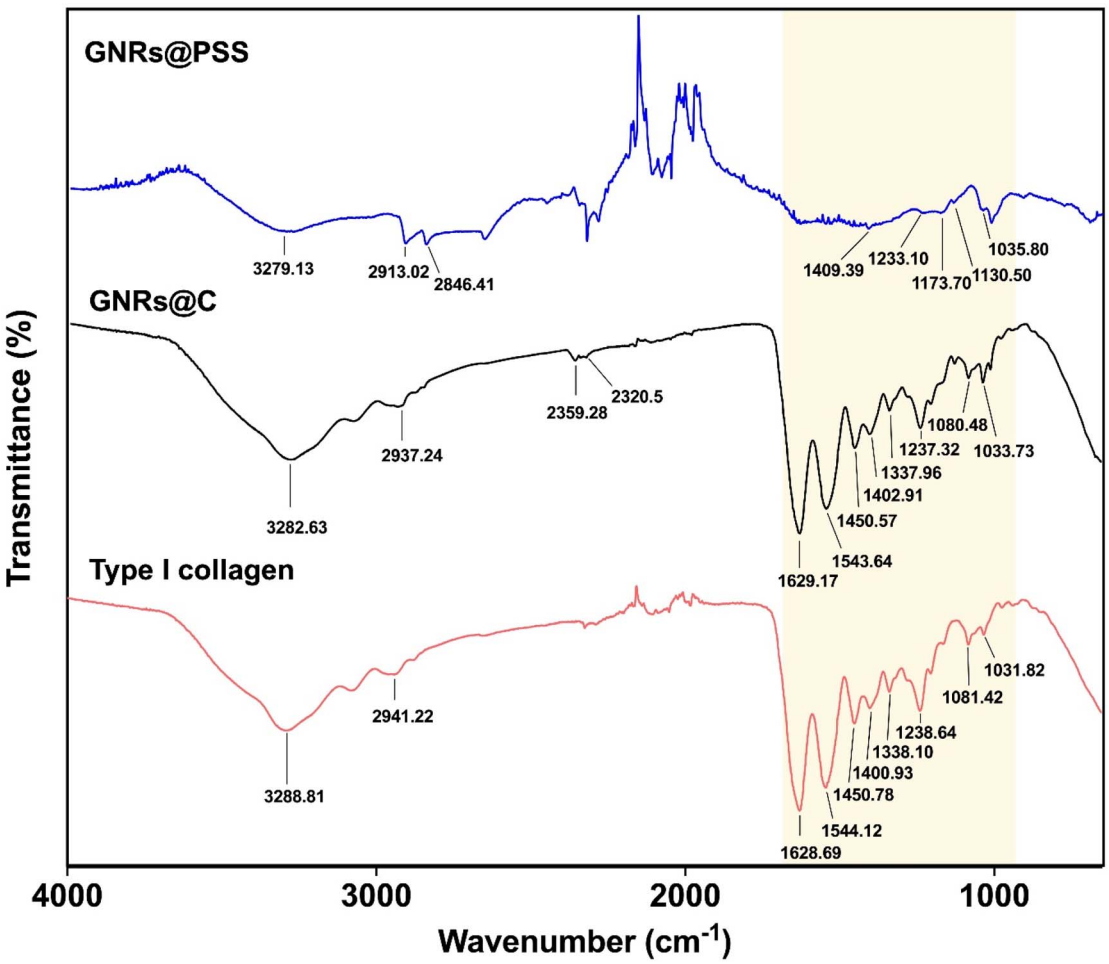


Fig. 3 FTIR spectra of GNRs@PSS, GNRs@C, and type I collagen.

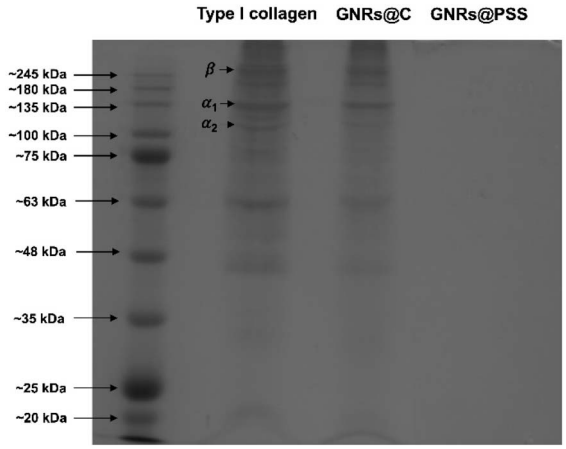


Fig. 4 Gel electrophoresis of type I collagen, GNRs@C, and GNRs@PSS.

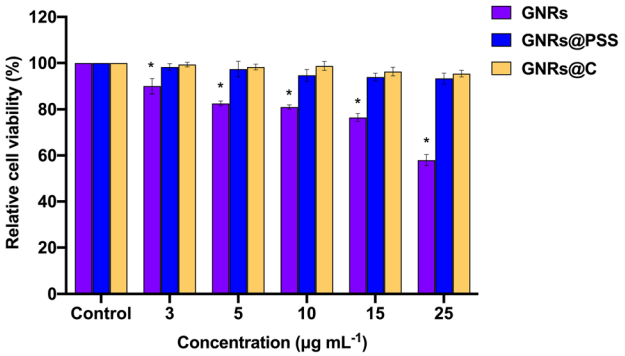


Fig. 5 Viability of HSF cells after treating with GNRs, GNRs@PSS, and GNRs@C at concentrations of 3, 5, 10, 15, and 25 μg $mL^{-1}$ for 24 h. *Significant difference in cell viability in comparison with control cells (untreated cells) and cells treated with GNRs@PSS, and GNRs@C at $P < 0.05$, $n \geq 4$.

negative zeta potential of gold nanoparticles changed to a positive value after decorating the surface of gold nanoparticles with collagen.

FTIR measurements were also used to confirm the surface modification of the GNRs with type I collagen. In this study, we investigated the FTIR spectra of GNRs@PSS, GNRs@C, and type I collagen (Fig. 3). The major characteristic amide peaks — amide I (1628.69 $cm^{-1}$), II (1544.12 $cm^{-1}$), and III (1238.64 $cm^{-1}$) — were detected in type I collagen. These peaks confirmed the integrity of the proteins in the collagen molecules.[33] The amide A and B peaks were detected at 3288.81 $cm^{-1}$ and 2941.22 $cm^{-1}$ respectively.[34]

The FTIR spectrum of GNRs@PSS showed the peak at 1035.80 $cm^{-1}$, which was attributed to symmetric stretching vibration. The S=O asymmetric stretching peaks at 1173.7 $cm^{-1}$ and 1233.10 $cm^{-1}$ were also detected in GNRs@PSS.[35] When GNRs@PSS were coated with type I collagen (GNRs@C), the peak at 3282.63 $cm^{-1}$ generating from the N–H stretching vibration of collagen was detected.[36] Many peaks detected in type I collagen were also detected in GNRs@C but not in GNRs@PSS. Furthermore, the protein peak at ~1450 $cm^{-1}$ caused by C–H bending[33] was also present in type I collagen and GNRs@C. These results confirmed that GNRs@PSS were successfully coated with type I collagen.

Gel electrophoresis was another technique used to confirm the presence of type I collagen on the surface of GNRs@PSS. As shown in Fig. 4, two different alpha chain bands were detected in type I collagen. These bands corresponded to α1 (molecular weight ~130 kDa) and α2 (molecular weight ~115 kDa) proteins. Similar findings were reported by Han *et al.*[37] Furthermore, a band of the β chain was also detected (molecular weight ~250 kDa).[38] The protein bands of GNRs@C were the same as those detected in type I collagen. This strongly indicates that the binding of type I collagen to GNRs@PSS was achieved. This binding occurred-through an electrostatic interaction. As expected, no protein bands were detected in GNRs@PSS.

### Investigation of HSF viability after treating with GNRs, GNRs@PSS, and GNRs@C

It is well-known that the cationic detergent, CTAB, which is commonly used as a stabilizer on GNR surfaces, is toxic to cells. In our previous work, we investigated the cytotoxicity of different surface modifications of GNRs in comparison to the original surface (CTAB) of GNRs. It clearly demonstrated that the CTAB on the surface of GNRs caused much higher toxicity to the cells than that of surface-modified GNRs.[27] Therefore, after successfully modifying the surface of GNRs, the cytotoxicity of GNRs@PSS and GNRs@C was assessed in HSF cells. After conducting a 24 h treatment of HSF cells with original GNRs (extra CTAB removal by centrifugation), GNRs@PSS, and GNRs@C at concentrations of 3, 5, 10, 15, and 25 μg $mL^{-1}$, it was evident that the surface modification of GNRs strongly reduced the cytotoxicity of GNRs. As shown in Fig. 5, the viabilities of HSF cells treated with GNRs at concentrations of 3, 5, 10, 15, and 25 μg $mL^{-1}$ were 89.95 ± 2.17, 82.56 ± 0.89, 81.05 ± 0.69, 76.48 ± 1.29, and 57.97 ± 1.82%, respectively. According to ISO 10993-5, cell viability percentages above 80% are considered as non-cytotoxicity.[39]

Our results showed that GNRs at concentrations ≥15 μg $mL^{-1}$ were toxic to HSF cells. The toxicity of GNRs was from CTAB stabilizing on the surface of GNRs.[27,40] When the surface of GNRs was modified with PSS (GNRs@PSS), the viabilities of HSF cells treated with different concentrations of GNRs@PSS were significantly higher than those of the original GNRs (98.24 ± 1.37, 97.38 ± 2.54, 94.65 ± 1.80, 93.88 ± 1.41, and 93.30 ± 1.53% for GNRs@PSS 3, 5, 10, 15, and 25 μg $mL^{-1}$, respectively). These results strongly indicate that PSS increases the biocompatibility of GNRs. After GNRs@PSS were coated with type I collagen (GNRs@C), the viabilities of HSF cells treated with 3, 5, 10, 15, and 25 μg $mL^{-1}$ GNRs@C were 99.33 ± 0.84, 98.28 ± 0.99, 98.71 ± 1.17, 96.28 ± 1.13, and 95.39 ± 0.76%, respectively. Modifying the surface of GNRs@PSS with type I collagen resulted in a slight improvement in HSF cell viability compared with GNRs@PSS.

### Investigation of HSF viability after treating with GNRs@PSS, and GNRs@C with and without LED irradiation

At the same concentration, GNRs were more toxic to HSF cells than GNRs@PSS and GNRs@C; therefore, we extensively investigated the effect of LED irradiation on HSF cells treated with GNRs@PSS and GNRs@C (at concentrations of 3, 5, 10, 15, and 25 μg $mL^{-1}$). HSF cells were treated separately with GNRs@PSS or GNRs@C for 5 h, followed by 5 min of LED exposure and then incubated for 24 h, clearly showing that the LED exposure significantly reduced the viability of HSF cells treated with 10, 15, and 25 μg $mL^{-1}$ GNRs@PSS (Fig. 6(a)). In contrast, as shown in Fig. 6(b), the viability of HSF cells treated with 10, 15, and 25 μg $mL^{-1}$ GNRs@C plus LED irradiation increased. Nevertheless, the viabilities of HSF cells treated with 3, 5, 10, 15, and 25 μg $mL^{-1}$ GNRs@PSS with and without LED irradiation were considered non-toxic because their viabilities were higher than 80% (Fig. 6(b)). Based on the results of this investigation, PSS and collagen did not induce toxicity in fibroblast cells. The biocompatibility of PSS- or collagen-coated gold nanoparticles has also been reported.[27,41]

The difference in the percentage of HSF viability after treatment with GNRs@PSS and GNRs@C may be due to variations in the surface plasmon resonances between GNRs@PSS and GNRs@C. The LED wavelength was ~638 nm, closely matching the LSPR of GNRs@PSS (~644 nm), leading to effective photothermal conversion. The longitudinal peak of GNRs@C was ~658 nm, which is longer than the wavelength of the LEDs. Consequently, the light absorption of GNRs@C was lower than that of GNRs@PSS resulting in a cell viability exceeding 97%. Overall, the use of GNRs@PSS and GNRs@C (3–25 μg $mL^{-1}$) with/without LED irradiation was not toxic to HSF cells.

The viabilities of HSF cells treated with GNRs@C (10, 15, and 25 μg $mL^{-1}$) and exposed to LED irradiation were slightly higher than those without LED irradiation. As mentioned previously, GNRs@C generated a weaker photothermal response due to its less efficient light absorption than GNRs@PSS. This allowed the LED light to primarily serve as a low-level photobiomodulation stimulus, thereby enhancing cellular activity without causing stress. An increase in cell viability after exposure to 600 nm light was reported by Tang *et al.*[42] It has been reported that a low level of ROS participating in cellular ROS homeostasis might increase cell viability.[43] Furthermore, cellular functions and cell biologics stimulated by low intensity light ranging from 630–1000 nm have been reported.[44,45]

### Cell proliferation of HSF viability after treating with GNRs@PSS and GNRs@C with and without LED irradiation

As shown in the previous section, LED irradiation of HSF cells treated with GNRs@C slightly increased the viability of HSF cells but did not induce viability in HSF cells treated with

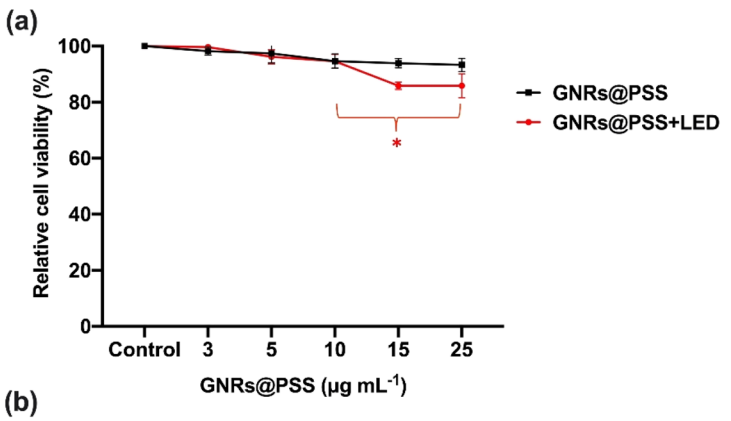


| GNRs@PSS (μg $mL^{-1}$) | No LED Cell viability (%) | LED Cell viability (%) |
|---|---|---|
| 0 | 100.00 ± 0.00 | 100.00 ± 0.00 |
| 3 | 98.24 ± 1.37 | 99.65 ± 1.19 |
| 5 | 97.38 ± 2.54 | 96.17 ± 1.91 |
| 10 | 94.65 ± 1.80 | 94.60 ± 2.34 |
| 15 | 93.88 ± 1.41 | 85.85 ± 0.84 |
| 25 | 93.30 ± 1.53 | 85.86 ± 2.26 |

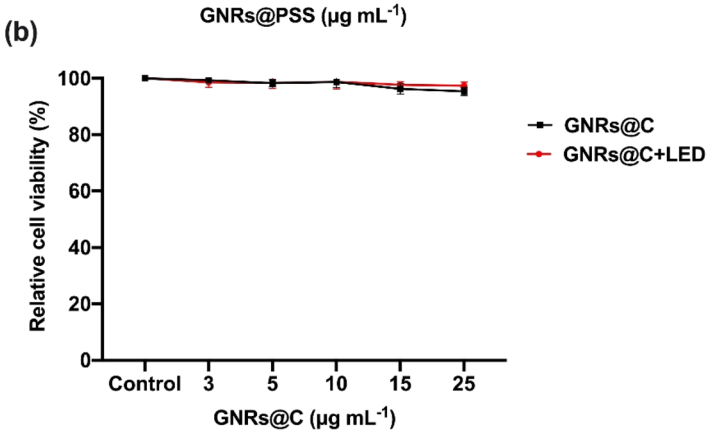


| GNRs@C (μg $mL^{-1}$) | No LED Cell viability (%) | LED Cell viability (%) |
|---|---|---|
| 0 | 100.00 ± 0.00 | 100.00 ± 0.00 |
| 3 | 99.33 ± 0.84 | 98.56 ± 1.31 |
| 5 | 98.28 ± 0.99 | 98.39 ± 1.69 |
| 10 | 98.71 ± 1.71 | 98.79 ± 1.77 |
| 15 | 96.28 ± 1.13 | 97.70 ± 0.68 |
| 25 | 95.39 ± 0.76 | 97.39 ± 0.66 |

Fig. 6 Viability of HSF cells treated with (a) GNRs@PSS and (b) GNRs@C (concentrations of 0, 3, 5, 10, 15, and 25 μg $mL^{-1}$) under LED irradiation and non-LED irradiation and then incubated for 24 h. *Significant difference in cell viability when HSF cells were treated with 10, 15, and 25 μg $mL^{-1}$ GNRs@PSS plus LED irradiation, compared with control cells (untreated) and control cells treated with LED irradiation at $P < 0.05$, $n \geq 4$.

GNRs@PSS. We therefore further investigated the proliferation of HSF cells treated with GNRs@PSS and GNRs@C, with and without LED irradiation. In this case, we only investigated the viability of HSF cells after treatment with GNRs@PSS or GNRs@C at a concentration of 3 μg $mL^{-1}$ because it provided the highest viability of HSF cells. After 24 h of incubation, the proliferation percentages of HSF cells treated with 3 μg $mL^{-1}$ GNRs@PSS with and without LED irradiation were 102.86 ± 1.90 and 101.53 ± 1.95%, respectively. The proliferation percentages of HSF cells at 48 h after treating with 3 μg $mL^{-1}$ GNRs@PSS under the same condition as of 24 h were 100.94 ± 2.79% (without LED irradiation) and 101.23 ± 3.76% (with LED irradiation). A small induction of cell proliferation was detected after HSF cells treated with GNRs@PSS were exposed to laser irradiation (Fig. 7(a and b)).

When HSF cells were treated with 3 μg $mL^{-1}$ GNRs@C, at 24 h incubation time the cell proliferations of HSF cells treated with GNRs@C without or with LED irradiation were 100.98 ± 2.37 and 104.08 ± 2.96%, respectively. At 48 h, the proliferations of HSF cells treated with GNRs@C were 103.92 ± 1.97% (without LED irradiation) and 107.82 ± 3.25% (with LED irradiation), respectively. Significant induction of HSF proliferation was observed in HSF cells treated with GNRs@C plus LED irradiation (Fig. 7(a and b)), indicating that this combined treatment effectively promoted the proliferation of HSF cells. It was reported that LEDs can activate intercellular signaling pathways that are related to proliferation and tissue regeneration resulting in enhancing cell proliferation.[13] Kim *et al.*[46] also demonstrated that red LEDs optimally enhanced cell proliferation in fibroblast-like cells (L929; mouse fibroblasts and human gingival fibroblasts) after irradiation at an energy density of 6.6 J $cm^{-2}$ and 2.55 J $cm^{-2}$ for L929 and human gingival fibroblasts, respectively.

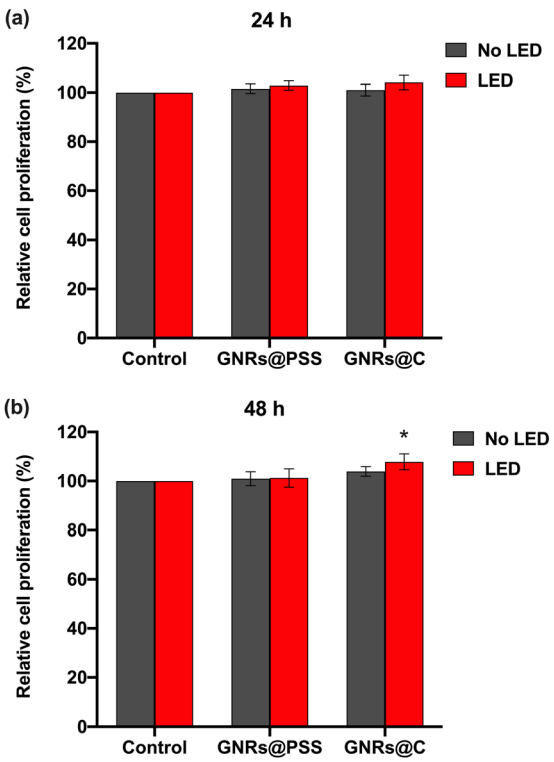


Fig. 7 Cell proliferations of HSF cells treated with GNRs@PSS and GNRs@C (3 μg $mL^{-1}$) under LED irradiation and non LED irradiation and then incubated for (a) 24 h and (b) 48 h. * denotes significant difference in cell proliferation compared with scratched HSF cells with/without LED irradiation ($P < 0.05$; $n \geq 5$).

Thus, it appears that different cell types require different energy densities to enhance cell proliferation. In our study, we found that an energy density of 2.08 J $cm^{-2}$ in combination with GNRs@C significantly induced HSF proliferation when compared with HSF cells without any treatment or HSF cells treated with 2.08 J $cm^{-2}$ LED irradiation alone. Our results suggest that GNRs@C with LED irradiation at a lower energy density than that previously reported[46] effectively enhanced cell proliferation. A possible mechanism by which LED irradiation enhances cell proliferation is through the interaction between light and cytochrome c oxidase in the mitochondrial respiratory chain. Cytochrome c oxidase is the primary cellular chromophore responsible for light absorption. An increase in the activity of this enzyme leads to elevated intracellular levels of ATP, cyclic adenosine monophosphate (cAMP), and ROS.[47] These signalling molecules then initiate a series of events resulting in cell proliferation by activating or inhibiting signalling molecules within the cytoplasm, which in turn triggers downstream cascades. Ultimately, these cascades lead to the synthesis of deoxyribonucleic acid (DNA), ribonucleic acid (RNA), proteins, and enzymes in various cellular components such as the cytoplasm, plasma membrane, and nucleus.[48] The effect of type I collagen in cell proliferation induction was also reported by Wang *et al.*[49]

### Ki-67 detection

Ki-67 is a protein that is widely used as a marker for cell proliferation.[50,51] In this study, we also investigated the appearance of Ki-67 protein in scratched HSF cells treated with GNRs@PSS and GNRs@C with/without LED irradiation. Scratched HSF cells were treated with GNRs@PSS or GNRs@C for 5 h, followed by exposure to LED irradiation for 5 min. Next, the scratched HSF cells were incubated for 48 h. After incubation, the treated cells were stained with Ki-67 using immunocytochemistry approach. The Ki-67 fluorescent signals were observed in cell nuclei (Fig. 8(a–f)) because the Ki-67 protein is associated with cell proliferation.[52,53] As shown in Fig. 8f, a strong green fluorescent staining of Ki-67 protein was detected in the nucleus of scratched HSF cells treated with GNRs@C plus LED irradiation. This result was in the same direction as the previous result (Fig. 7) that the proliferation of scratched HSF cells was enhanced after treatment with GNRs@C and then LED irradiation. In contrast, in the absence of LED irradiation, few cell nuclei were stained with green fluorescence (Fig. 8c). These findings indicate that stabilization of type I collagen on the surface of GNRs, in combination with LED, promoted the proliferation of scratched HSF cells. The induction of Ki-67 protein levels by type I collagen has also been reported previously.[54] In addition, Li *et al.*[55] reported that LED irradiation at a wavelength of 630 nm induced Ki-67 expression in skin

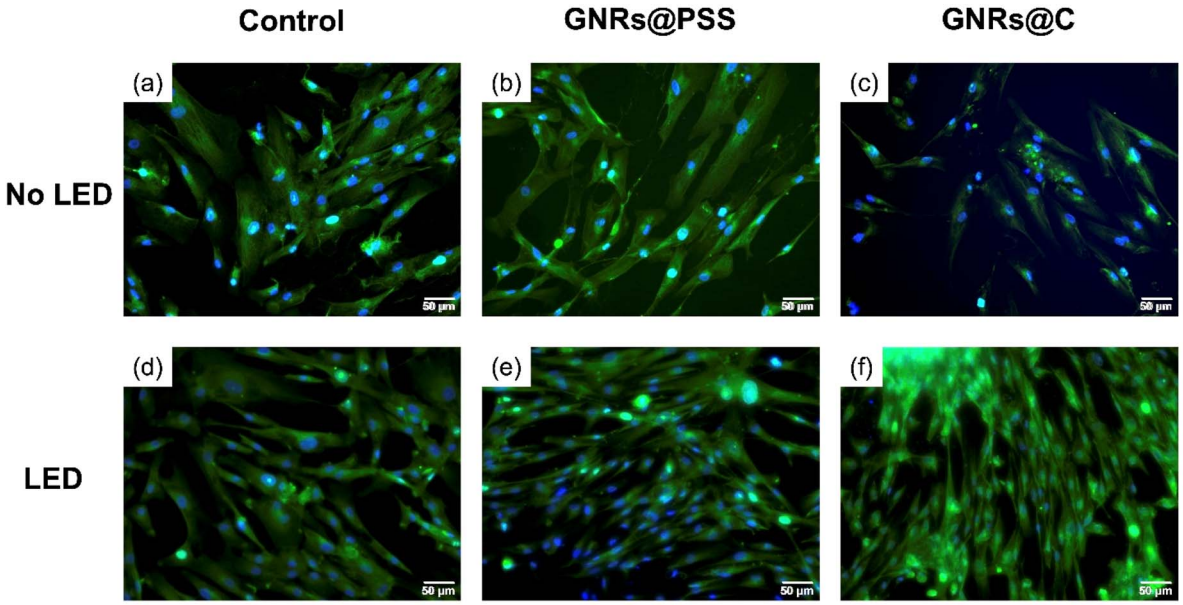


Fig. 8 Images of scratched HSF cells under different conditions, immunofluorescently labelled for Ki-67 (green fluorescence in the cell nuclei). (a) Scratched HSF cells without any treatment, (b) treated with GNRs@PSS, (c) treated with GNRs@C, (d) treated with LED irradiation, (e) treated with GNRs@PSS and LED irradiation, and (f) treated with GNRs@C and LED irradiation.

lesions. However, the role of type I collagen in the induction of Ki-67 expression is not fully understood. Nevertheless, LED irradiation may potentially influence the increase in mitochondrial activity, consequently leading to the induction of Ki-67 expression, as reported by Umino *et al.*[56]

### Cellular uptake of GNRs@PSS, and GNRs@C by scratched HSF cells irradiated with LEDs

The cellular uptake of GNRs@PSS and GNRs@C by scratched HSF cells was investigated. Scratched HSF cells were treated with 3 μg $mL^{-1}$ GNRs@PSS or GNRs@C for 5 h, exposed to LED irradiation for 5 min, and further incubated for 24 and 48 h. As shown in Fig. 9, the gold concentrations detected in scratched HSF cells treated with GNRs@C plus LED irradiation (1.03 ± 0.22 μg $L^{-1}$) and then incubated for 24 h was significantly higher than that of GNRs@PSS plus LED irradiation (0.11 ± 0.07 μg $L^{-1}$). As expected, similar results were observed after 48 h of incubation. Scratched HSF cells were treated with 3 μg $mL^{-1}$ GNRs@C plus LED irradiation (1.06 ± 0.30 μg $L^{-1}$) had a higher gold content than GNRs@PSS plus LED irradiation (0.23 ± 0.06 μg $L^{-1}$). These results indicate that type I collagen at the surface of GNRs induced the cellular uptake of GNRs@C. Similar results were also reported in our previous work,[41] where we found that type I collagen can enhance particle adhesion and cellular internalization. The zeta potential of particles should play a vital role in an interaction between cell membrane and particles. As mentioned previously, the zeta potential of the GNRs@C was 20.70 ± 0.55 mV. In contrast, a negative value was detected in GNRs@PSS (−43.43 ± 0.75 mV). There was no significant difference in the cellular uptake of GNRs@PSS after 24 and 48 h of incubation (Fig. 9). Comparable findings were also reported in the research conducted by Xiao *et al.*[57] Their study showed that positively charged GNRs were taken up by cells more than negatively charged GNRs.[57] Studies by Hauck *et al.*[58] and Pissuwan *et al.*[27] have demonstrated the same trends. Based on these results, the zeta potential of nanoparticles demonstrated a significant influence on cellular uptake.

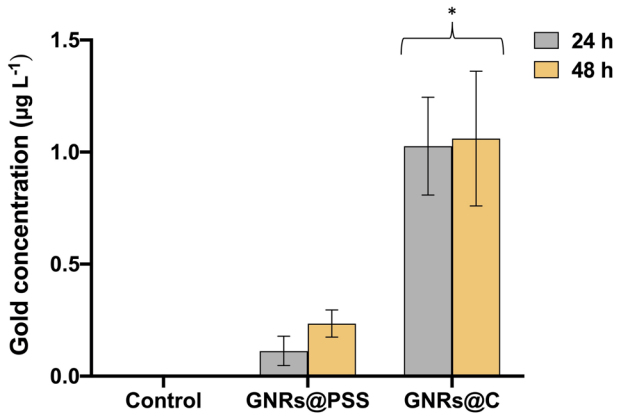


Fig. 9 Gold contents in scratched HSF cells incubated with 3 μg $mL^{-1}$ of GNRs@PSS and GNRs@C for 5 h and then exposed to LED irradiation for 5 min, followed by 24 and 48 h of incubation. * Denotes a significant difference in cellular uptake of scratched HSF cells compared with control and scratched HSF cells treated with GNRs@PSS for the same incubation period ($P < 0.05$; $n \geq 3$).

The cellular uptake of scratched HSF cells treated with GNRs@PSS, LED irradiation, and 48 h incubation (0.23 ± 0.06 μg $L^{-1}$) was higher than that of the cells incubated for 24 h (0.11 ± 0.07 μg $L^{-1}$). Nevertheless, this difference was not statistically significant. In the case of scratched HSF cells treated with GNRs@C and LED irradiation, the cellular uptakes of GNRs@C at 24 and 48 h were similar (Fig. 9).

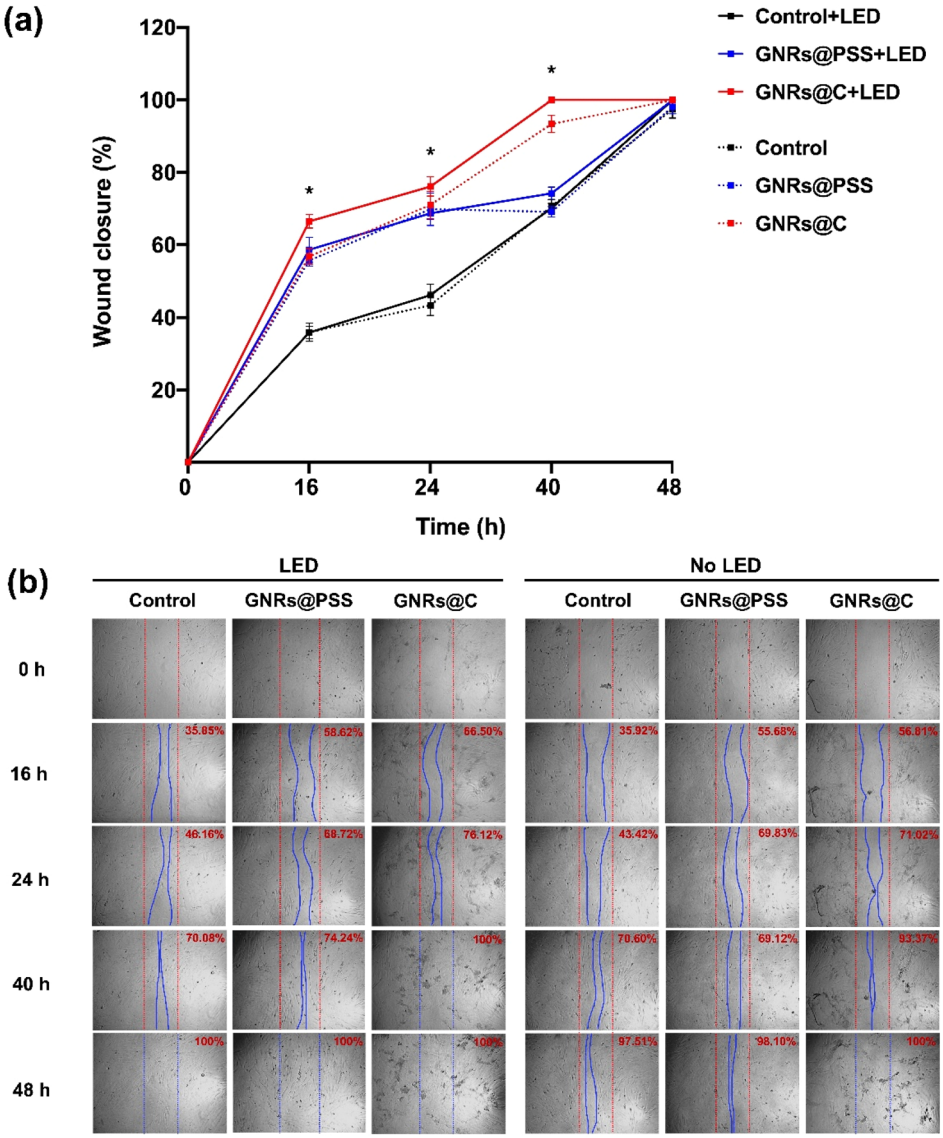


Fig. 10 (a) Percentages of wound closure in scratched HSF cells treated with 3 μg $mL^{-1}$ GNRs@PSS and GNRs@C with/without LED irradiation for 0, 16, 24, 40, and 48 h.*Significant difference in wound closure compared with the control sample (untreated HSF cells). ($P < 0.05$; $n \geq 3$). (b) Images of scratched HSF cell migration of scratched HSF cells treated with 3 μg $mL^{-1}$ GNRs@PSS and GNRs@C with/without LED irradiation 0, 16, 24, 40, and 48 h.

### Effect of GNRs@PSS and GNRs@C with or without LED irradiation on wound closure

The wound scratch assay was conducted to investigate the healing activity of scratched HSF cells *in vitro*. Scratched HSF cells were treated with 3 μg $mL^{-1}$ GNRs@PSS and GNRs@C for 5 h, followed by LED irradiation for 5 min, and then incubated for 0, 16, 24, 40, and 48 h. The percentages of wound closure in scratched HSF cells treated with GNRs@PSS plus LED irradiation and incubated for 16, 24, 40, and 48 h were 58.62 ± 3.44, 68.72 ± 1.75, 74.24 ± 1.72, and 100%, respectively (Fig. 10(a and b)). When scratched HSF cells treated with GNRs@PSS without LED irradiation, the percentages of wound closure after incubation for 16, 24, 40, and 48 h were 55.68 ± 1.55, 69.83 ± 4.49, 69.12 ± 1.40, and 98.10 ± 1.90%. After 16 h of incubation, the percentages of wound closure in scratched HSF cells treated with GNRs@C were 66.50 ± 1.84% (with LED irradiation) and 56.81 ± 2.14% (without LED irradiation). The percentages of wound closure in scratched HSF cells treated with GNRs@C were 76.12 ± 2.64% (with LED irradiation) and 71.02 ± 3.73% (without LED irradiation) after 24 h incubation. After 40 h, the full wound closure was observed in scratched HSF cells treated with GNRs@C plus LED irradiation. However, the percentage of wound closure of scratched HSF cells treated with GNRs@C without LED irradiation was 93.37 ± 2.40% after 40 h of incubation and full wound closure appeared after 48 h of incubation. These results demonstrated that GNRs@C and LED irradiation effectively enhanced wound closure. In the case of scratched HSF cells without any treatment, after 48 h of

incubation the percentage of wound closure was 97.51 ± 2.49%. The percentages of wound closure lower than 75% were found in untreated scratched HSF cells at 16 (35.92 ± 2.50%), 24 (43.42 ± 2.85%), and 40 h (70.60 ± 1.86%). When scratched HSF cells were exposed to the LED irradiation, the percentages of wound closure after 16, 24, 40, and 48 h were 35.85 ± 1.72, 46.16 ± 2.94, 70.08 ± 1.34, and 100%, respectively. Nevertheless, no significant difference was observed in the percentage of wound closure between scratched HSF cells with and without LED irradiation at the same post-wounding time points (Fig. 10).

The wound closure results were in the same direction as that of the cell proliferation results. The combination of GNRs@C and LED irradiation most effectively enhanced the healing of scratched HSF cells. As per our previous study published in,[41] type I collagen enhanced cell migration by guiding cell adhesion and migration. The molecular mechanism of cell migration after treating with collagen can occur through PI3k/Akt/mTOR signaling pathway.[59] Therefore, type I collagen has been applied in wound healing applications.[60] It has been reported that LED light can be absorbed by cytochrome c oxidase leading to the dissociation of nitric oxide inhibition. Furthermore, LED light can increase energy metabolism, including respiratory rate, enzyme activity, and transcription factor expression, which are associated with cellular activities resulting in enhanced cell proliferation, migration, and adhesion.[13,15]

### Effect of GNRs@PSS and GNRs@C with or without LED irradiation on inflammatory cytokines response and angiogenesis growth factors

Inflammatory cytokines (IL-6 and TNF-α) were examined after scratched HSF cells were treated with 3 μg mL$^{-1}$ GNRs@PSS or GNRs@C with or without LED irradiation and then incubated for 48 h. We focused on these two inflammatory cytokines because they play a major role in wound healing. The results showed that the concentration of IL-6 in scratched HSF cells treated with GNRs@C plus LED irradiation significantly decreased from 131.41 ± 4.25 pg mL$^{-1}$ (HSF cells without any treatment; control) to 96.57 ± 2.41 pg mL$^{-1}$ (Fig. 11(a)). In the case of scratched HSF cells treated with 3 μg mL$^{-1}$ GNRs@C without LED irradiation, the IL-6 concentration was 129.51 ± 5.71 pg mL$^{-1}$, which was similar to the control cells (Fig. 11(a)). This indicates that without LED irradiation GNRs@C had no effect on IL-6 reduction. Furthermore, the presence of GNRs@C did not stimulate an increase in IL-6 production in scratched HSF cells.

Similar to GNRs@C, the IL-6 concentration in scratched HSF cells treated with GNRs@PSS plus LED irradiation was reduced to 122.96 ± 2.09 pg mL$^{-1}$. In the case of without LED irradiation, scratched HSF cells treated with 3 μg mL$^{-1}$ GNRs@PSS had IL-6 concentration at 127.94 ± 2.35 pg mL$^{-1}$. GNRs@C and GNRs@PSS with LED irradiation reduced IL-6 production in scratched HSF cells more effectively than without LED irradiation. However, when scratched HSF cells were treated with GNRs@PSS and GNRs@C, followed by LED irradiation, the IL-6

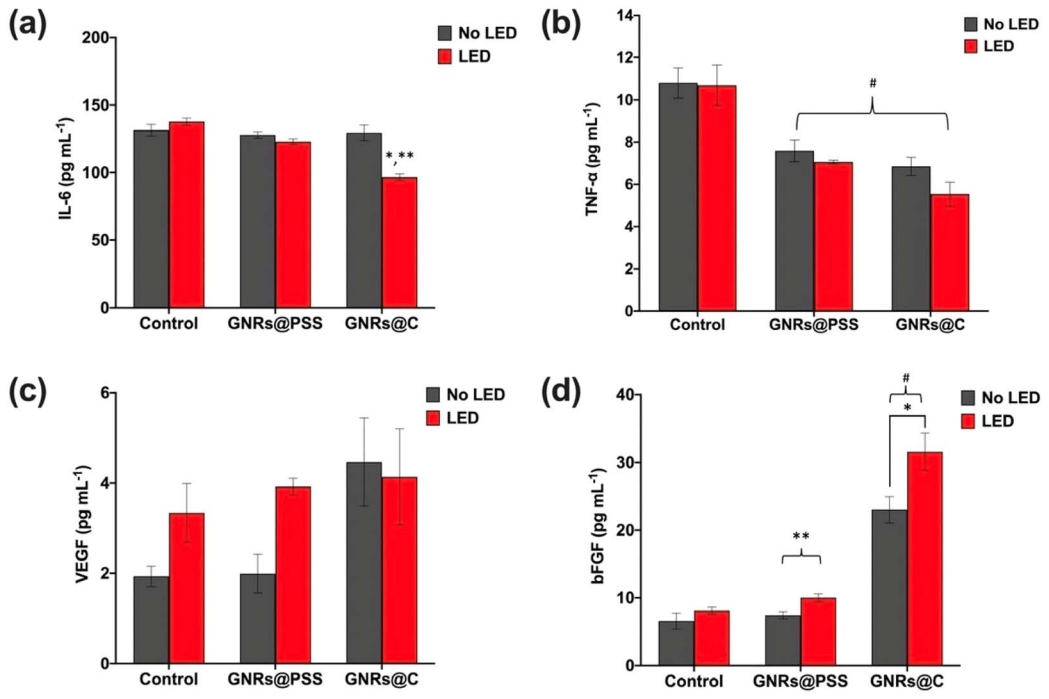


Fig. 11 Levels of (a) IL-6, (b) TNF-α, (c) VEGF, and (d) bFGF in scratched HSF cells treated with GNRs@PSS and GNRs@C with/without irradiation at 48 h post-wounding. In (a), * denotes a significant difference compared to scratched HSF cells with/without LED irradiation and ** denotes a significant difference compared to scratched HSF cells treated with GNRs@PSS plus LED irradiation. In (b), # denotes a significant difference compared to scratched HSF cells with/without LED irradiation. In (d), * denotes a significant difference in scratched HSF cells with GNRs@C with/without LED irradiation, ** denotes a significant difference compared to scratched HSF cells treated with GNRs@C with/without LED irradiation, # denotes a significant difference compared to control scratched HSF cells with/without LED irradiation ($P < 0.05$; $n \geq 3$).

levels in cells treated with GNRs@C was significantly lower than that of GNRs@PSS (Fig. 11(a)). The IL-6 concentration in scratched HSF cells exposed to LED irradiation was 137.77 ± 2.67 pg $mL^{-1}$, which was not significantly different from that in scratched HSF cells without LED irradiation (131.41 ± 4.25 pg $mL^{-1}$). Our findings demonstrated that scratched HSF cells exposed to 3 μg $mL^{-1}$ GNRs@C and LED irradiation exhibited the lowest IL-6 concentration at 48 h post-wounding, as illustrated in Fig. 11(a). The reduction of IL-6 during wound healing was also observed in our previous work[41] and in the work reported by Wang *et al.*[61]

As shown in Fig. 11(b), the lowest concentration of TNF-α at 48 h post-wounding was also detected in scratched HSF cells treated with 3 μg $mL^{-1}$ GNRs@C plus LED irradiation (5.53 ± 0.58 pg $mL^{-1}$). The concentration of TNF-α in scratched HSF cells treated with GNRs@C without LED irradiation was 6.85 ± 0.43 pg $mL^{-1}$. When scratched HSF cells treated with GNRs@PSS, the concentrations of TNF-α were 7.06 ± 0.09 pg $mL^{-1}$ for LED irradiation and 7.59 ± 0.51 pg $mL^{-1}$ for non-LED irradiation. Concentrations of TNF-α in scratched HSF cells with and without LED irradiation were 10.69 ± 0.96 and 10.80 ± 0.71 pg $mL^{-1}$, respectively. Our results show that GNRs@C and GNRs@PSS with/without LED irradiation significantly affected on reduction of TNF-α levels.

IL-6 and TNF-α play crucial roles in various stages of wound healing. Nevertheless, excessive production of these cytokines can lead to a prolonged inflammatory phase, which negatively affects the healing process.[62,63] Our results showed that significant decreases of IL-6 and TNF-α were observed in scratched HSF cells treated with GNRs@C and LED irradiation. Although GNRs@PSS plus LED irradiation also reduced the level of TNF-α (7.06 ± 0.09 pg $mL^{-1}$), scratched HSF cells treated with GNRs@C plus LED irradiation had lower TNF-α levels (5.53 ± 0.58 pg $mL^{-1}$) compared to GNRs@PSS plus LED irradiation. The higher cellular uptake of GNRs@C than that of GNRs@PSS could explain this phenomenon.

VEGF is a growth factor that contributes to fibroblast migration thorough the induction of angiogenesis and collagen production.[64,65] As shown in Fig. 11(c), the VEGF levels increased from 1.93 ± 0.23 pg $mL^{-1}$ (scratched HSF cells without any treatment) to 3.34 ± 0.65 pg $mL^{-1}$ (scratched HSF cells with LED irradiation). Similar to scratched HSF cells treated with GNRs@PSS and LED irradiation, the VEGF increased from 1.93 ± 0.23 pg $mL^{-1}$ to 3.92 ± 0.19 pg $mL^{-1}$. However, without LED irradiation, scratched HSF cells treated with GNRs@PSS had the VEGF concentration (1.99 ± 0.43 pg $mL^{-1}$) similar to scratched HSF cells without any treatment (1.93 ± 0.23 pg $mL^{-1}$). Interestingly, in the case of scratched HSF cells treated with GNRs@C, the VEGF concentrations were 4.47 ± 0.98 pg $mL^{-1}$ (without LED irradiation) and 4.14 ± 1.06 pg $mL^{-1}$ (with LED irradiation). This clearly demonstrated that both GNRs@C and LED treatment individually tended to induce VEGF production, although the increase was not statistically significant compared to the control cells (without any treatment). A similar outcome for the effect of LEDs on VEGF induction was reported by Cha *et al.*[66] Another finding reported by Kuppa *et al.*[67] also demonstrated that the red-light LED (at a wavelength of ~630 nm) can induce VEGF production in fibroblast cells. However, the combination of GNRs@C and LED irradiation did not have a significant effect on increasing the levels of VEGF compared to stand alone GNRs@C or LED irradiation.

bFGF is another growth factor that is involved in wound healing. It can promote the migration and proliferation of fibroblast cells.[68] As shown in Fig. 11(d), the bFGF concentrations of scratched HSF cells with/without LED irradiation were 8.13 ± 0.51 and 6.58 ± 1.19 pg $mL^{-1}$, respectively. The bFGF concentrations of scratched HSF cells treated with GNRs@PSS with/without LED irradiation were 10.02 ± 0.58 and 7.45 ± 0.51 pg $mL^{-1}$, respectively. The high concentrations of bFGF were observed in scratched HSF cells treated with GNRs@C plus LED irradiation (31.59 ± 2.71 pg $mL^{-1}$) and with GNRs@C alone (23.00 ± 1.93 pg $mL^{-1}$). Based on our results, all treatment conditions with LED irradiation resulted in higher bFGF levels compared to those without LED irradiation. A previous study by Stavri *et al.*[69] reported that bFGF can indirectly induce VEGF expression. Therefore, an increase in VEGF levels can also be an indirect effect of bFGF induction in scratched HSF cells under treatment conditions involving LED irradiation. In addition to LED irradiation, the combination of type I collagen and GNRs contributed to the induction of VEGF and bFGF levels, as reported in our previous study.[41]

In comparison to GNRs@PSS, the application of GNRs@C to scratched HSF cells markedly elevated the bFGF levels. This indicates that type I collagen on the surface of GNRs could induce the production of bFGF. However, the mechanism of this induction is not yet known. According to Dierckx *et al.*,[70] the use of collagen peptides in the treatment of human dermal fibroblast cells has been shown to stimulate fibroblast cell proliferation and collagen synthesis, thereby enhancing tissue regeneration. Furthermore, Felician *et al.*,[71] reported that collagen can enhance wound healing activity. Kusnadi *et al.*[72] also discussed the role of collagen on the surface of metal nanoparticles in forming extracellular matrix, which aids in cell proliferation and stimulates the healing process.

Based on our results, an increase in VEGF and bFGF levels compared to control cells signify increased angiogenic activity, which is essential in the wound healing process, particularly for supplying nutrients and oxygen to regenerating tissues. Notably, bFGF plays a significant role in promoting the migration and proliferation of fibroblast. These synergistic effects of GNRs@C and LED irradiation suggest that a microenvironment favorable for wound healing enhancement was created. The ability of nanomaterials to stimulate the gene expression related to angiogenic effects was also reported by Liu *et al.*[73] Taken together, our findings suggest that GNRs@C and LED irradiation can significantly enhance the wound healing process.

## Conclusion

Our findings clearly demonstrate that the combination of GNRs@C and LED irradiation produces a synergistic effect that significantly enhances wound healing in scratched HSF cells (100% wound closure at 40 h). This was further evidenced by

 

a substantial reduction in inflammatory cytokines (from 131.41 $\pm$ 4.25 pg mL$^{-1}$ to 96.57 $\pm$ 2.41 pg mL$^{-1}$ for IL-6 and from 10.80 $\pm$ 0.71 pg mL$^{-1}$ to 5.53 $\pm$ 0.58 pg mL$^{-1}$ for TNF-$\alpha$), which are known to impede the healing process when persistently elevated. Additionally, the combination treatment led to the highest production of bFGF, a key growth factor involved in tissue regeneration. These outcomes collectively indicate that GNRs@C combined with LED irradiation not only supports cellular viability but also actively stimulates cellular functions essential for wound repair. The strong experimental evidence supports the efficacy of this combined approach, underscoring its potential as a novel and promising therapeutic strategy in regenerative medicine. Future studies should focus on validating these findings in terms of antimicrobial activity and through *in vivo* models. Furthermore, the degradation of the collagen coating on the surface of GNRs should be investigated.

## Data availability

Data available within the article. The authors confirm that the data supporting the findings of this study are available within the article.

## Author contributions

S. P. conducted experiments, performed data analysis, prepared figures, and wrote the first draft of the manuscript. D. P. conceptualized this work, performed experimental design and data analysis, funding acquisition, revised and re-written the manuscript, visualization, validation, data curation, and supervised the work.

## Conflicts of interest

There are no conflicts to declare.

## Acknowledgements

This work received funding support from Mahidol University (Fundamental Fund: Fiscal Year 2023 by the National Science Research and Innovation Fund) (NSRF); Grant No. FF077/2566. The authors thank the School of Materials Science and Innovation and the Central Instrument Facility, Faculty of Science, Mahidol University, for providing the facilities used in this research. The authours also thank Ms. Felicie Duault for technical support.

## References

1 H. Chen, L. Shao, Q. Li and J. Wang, *Chem. Soc. Rev.*, 2013, **42**, 2679–2724.
2 D. Pissuwan, S. M. Valenzuela and M. B. Cortie, *Biotechnol. Genet. Eng. Rev.*, 2008, **25**, 93–112.
3 D. Salah, F. S. Moghanm, M. Arshad, A. A. Alanazi, S. Latif, M. I. El-Gammal, E. M. Shimaa and S. Elsayed, *Diagnostics*, 2021, **11**, 1196.
4 J. Wan, J.-H. Wang, T. Liu, Z. Xie, X.-F. Yu and W. Li, *Sci. Rep.*, 2015, **5**, 1–16.
5 M. E. d. A. Chaves, A. R. d. Araújo, A. C. C. Piancastelli and M. Pinotti, *An. Bras. Dermatol.*, 2014, **89**, 616–623.
6 A. Kushwaha, L. Goswami and B. S. Kim, *Nanomaterials*, 2022, **12**, 618.
7 S. Guo and L. A. DiPietro, *J. Dent. Res.*, 2010, **89**, 219–229.
8 N. N. Mahmoud, L. M. Al-Kharabsheh, E. A. Khalil and R. Abu-Dahab, *Nanomaterials*, 2019, **9**, 1131.
9 W. E. Soliman, H. S. Elsewedy, N. S. Younis, P. Shinu, L. E. Elsawy and H. A. Ramadan, *Polymers*, 2022, **14**, 2637.
10 G. B. Reddy, A. Madhusudhan, D. Ramakrishna, D. Ayodhya, M. Venkatesham and G. Veerabhadram, *J. Nanostructure Chem.*, 2015, **5**, 185–193.
11 S. Poomrattanangoon, A. Ounkaew, D. Pissuwan and R. Narain, *Langmuir*, 2024, **40**, 21795–21803.
12 W. Posten, D. A. Wrone, J. S. Dover, K. A. Arndt, S. Silapunt and M. Alam, *Dermatol. Surg.*, 2005, **31**, 334–340.
13 P. Avci, A. Gupta, M. Sadasivam, D. Vecchio, Z. Pam, N. Pam and M. R. Hamblin, *Semin. Cutaneous Med. Surg.*, 2013, **32**, 41–52.
14 X. Yi, Q.-Y. Duan and F.-G. Wu, *Research*, 2021, **2021**, 9816594.
15 A. Gupta, P. Avci, M. Sadasivam, R. Chandran, N. Parizotto, D. Vecchio, W. C. de Melo, T. Dai, L. Y. Chiang and M. R. Hamblin, *Biotechnol. Adv.*, 2013, **31**, 607–631.
16 D. Rana, K. Ramasamy, M. Leena, C. Jiménez, J. Campos, P. Ibarra, Z. S. Haidar and M. Ramalingam, *Biotechnol. Prog.*, 2016, **32**, 554–567.
17 H. B. Cotler, R. T. Chow, M. R. Hamblin and J. Carroll, *MOJ Orthop. Rheumatol.*, 2015, **2**, 188–194.
18 S. Farivar, T. Malekshahabi and R. Shiari, *J. Lasers Med. Sci.*, 2014, **5**, 58.
19 K. Yue, J. Nan, X. Zhang, J. Tang and X. Zhang, *Appl. Therm. Eng.*, 2016, **99**, 1093–1100.
20 G. Poorani, A. P. Rao, G. Singaravelu and E. Manickan, *J. Nanophotonics*, 2016, **10**, 026027.
21 A. L. Kwansa, R. De Vita and J. W. Freeman, *Biophys. Chem.*, 2016, **214–215**, 1–10.
22 C. Wiegand, U. Schönfelder, M. Abel, P. Ruth, M. Kaatz and U. C. Hipler, *Arch. Dermatol. Res.*, 2010, **302**, 419–428.
23 P. Buachan, L. Chularojmontri and S. K. Wattanapitayakul, *Nutrients*, 2014, **6**, 1618–1634.
24 C. Kim, S. S. Agasti, Z. Zhu, L. Isaacs and V. M. Rotello, *Nat. Chem.*, 2010, **2**, 962–966.
25 C. Graefe, L. Eichhorn, P. Wurst, J. Kleiner, A. Heine, I. Panetas, Z. Abdulla, A. Hoeft, S. Frede and C. Kurts, *Mol. Biol. Rep.*, 2019, **46**, 4631–4643.
26 A. K. Sahu, A. Das, A. Ghosh and S. Raj, *Nano Express*, 2021, **2**, 010009.
27 D. Pissuwan, Y. Kumagai and N. I. Smith, *Part. Part. Syst. Charact.*, 2013, **30**(5), 427–433.
28 H. J. Parab, H. M. Chen, T.-C. Lai, J. H. Huang, P. H. Chen, R.-S. Liu, M. Hsiao, C.-H. Chen, D.-P. Tsai and Y.-K. Hwu, *J. Phys. Chem. C*, 2009, **113**, 7574–7578.
29 H. Chen, X. Kou, Z. Yang, W. Ni and J. Wang, *Langmuir*, 2008, **24**, 5233–5237.

30 R. G. Rayavarapu, W. Petersen, L. Hartsuiker, P. Chin, H. Janssen, F. W. Van Leeuwen, C. Otto, S. Manohar and T. G. Van Leeuwen, *Nanotechnology*, 2010, **21**, 145101.
31 V. S. Cardoso, P. V. Quelemes, A. Amorin, F. L. Primo, G. G. Gobo, A. C. Tedesco, A. C. Mafud, Y. P. Mascarenhas, J. R. Corrêa and S. A. Kuckelhaus, *J. Nanobiotechnology*, 2014, **12**, 1–9.
32 A. Y.-H. Yu, R.-H. Fu, S.-h. Hsu, C.-F. Chiu, W.-H. Fang, C.-A. Yeh, C.-M. Tang, H.-H. Hsieh and H.-S. Hung, *Mater. Today Adv.*, 2021, **12**, 100191.
33 R. Sripriya and R. Kumar, *Food and Nutrition Sciences*, 2015, **6**, 1468–1478.
34 Z. I. Elbialy, A. Atiba, A. Abdelnaby, H. Al II, A. Elsheshtawy, H. A. El-Serehy, M. M. Abdel-Daim, S. E. Fadl and D. H. Assar, *BMC Vet. Res.*, 2020, **16**, 352.
35 S. A. Alex, N. Chandrasekaran and A. Mukherjee, *IET Nanobiotechnol.*, 2019, **13**, 522–529.
36 X. Xiang, F. Long, A. Narkar, R. E. Kinnunen, R. Shahbazian-Yassar, B. P. Lee and P. A. Heiden, *J. Appl. Polym. Sci.*, 2016, **133**, 42868.
37 Q.-Y. Han, T. Koyama, S. Watabe, Y. Nagashima and S. Ishizaki, *Molecules*, 2023, **28**, 889.
38 O. S. Rabotyagova, P. Cebe and D. L. Kaplan, *Mater. Sci. Eng., C*, 2008, **28**, 1420–1429.
39 J. López-García, M. Lehocký, P. Humpolíček and P. Sáha, *J. Funct. Biomater.*, 2014, **5**, 43–57.
40 S. Wang, W. Lu, O. Tovmachenko, U. S. Rai, H. Yu and P. C. Ray, *Chem. Phys. Lett.*, 2008, **463**, 145–149.
41 S. Poomrattanangoon and D. Pissuwan, *Heliyon*, 2024, **10**, e33302.
42 L. Tang, H. Qin, S. Lin and M. Liu, *Photonics*, 2023, **10**, 315.
43 J.-S. Kim and S.-T. S. Lim, *Curr. Issues Mol. Biol.*, 2022, **44**, 1235–1246.
44 K. D. Desmet, D. A. Paz, J. J. Corry, J. T. Eells, M. T. T. Wong-Riley, M. M. Henry, E. V. Buchmann, M. P. Connelly, J. V. Dovi, H. L. Liang, D. S. Henshel, R. L. Yeager, D. S. Millsap, J. Lim, L. J. Gould, R. Das, M. Jett, B. D. Hodgso n, D. Margolis and H. T. Whelan, *Photomed. Laser Surg*, 2006, **24**, 121–128.
45 J. T. Eells, M. T. T. Wong-Riley, J. VerHoeve, M. Henry, E. V. Buchman, M. P. Kane, L. J. Gould, R. Das, M. Jett, B. D. Hodgson, D. Margolis and H. T. Whelan, *Mitochondrion*, 2004, **4**, 559–567.
46 M.-S. Kim, Y.-I. Cho, M.-S. Kook, S.-C. Jung, Y.-H. Hwang and B.-H. Kim, *Int. J. Photoenergy*, 2015, 916838.
47 R. Zein, W. Selting and M. Hamblin, *J. Biomed. Opt.*, 2018, **23**, 120901.
48 L. F. de Freitas and M. R. Hamblin, *IEEE J. Sel. Top. Quantum Electron.*, 2016, **22**, 38–364.
49 D. Wang, F. Chang, Z. Guo, M. Chen, T. Feng, M. Zhang, X. Cui, Y. Jiang, J. Li, Y. Li and J. Yan, *Tissue Cell*, 2024, **90**, 102506.
50 V. Zorin, A. Zorina, N. Smetanina, P. Kopnin, I. V. Ozerov, S. Leonov, A. Isaev, D. Klokov and A. N. Osipov, *Aging*, 2017, **9**, 1404.
51 L. Remnant, N. Y. Kochanova, C. Reid, F. Cisneros-Soberanis and W. C. Earnshaw, *Open Biol.*, 2021, **11**, 210120.
52 K. Mrouj, N. Andrés-Sánchez, G. Dubra, P. Singh, M. Sobecki, D. Chahar, E. Al Ghoul, A. B. Aznar, S. Prieto, N. Pirot, F. Bernex, B. Bordignon, C. Hassen-Khodja, M. Villalba, L. Krasinska and D. Fisher, *Proc. Natl. Acad. Sci. U. S. A.*, 2021, **118**, e2026507118.
53 M. Sobecki, K. Mrouj, A. Camasses, N. Parisis, E. Nicolas, D. Llères, F. Gerbe, S. Prieto, L. Krasinska, A. David, M. Eguren, M.-C. Birling, S. Urbach, S. Hem, J. Déjardin, M. Malumbres, P. Jay, V. Dulic, D. L. J. Lafontaine, R. Feil and D. Fisher, *eLife*, 2016, **5**, e13722.
54 J. Furuzawa-Carballeda, O. A. Muñoz-Chablé, J. Barrios-Payán and R. Hernández-Pando, *Eur. J. Clin. Investig.*, 2009, **39**, 591–597.
55 Y. Li, J. Zhang, Y. Xu, Y. Han, B. Jiang, L. Huang, H. Zhu, Y. Xu, W. Yang and C. Qin, *PLoS One*, 2016, **11**, e0157898.
56 Y. Umino and M. Denda, *Sking Res. Technol.*, 2023, **29**, e13447.
57 Y. Xiao, W. Xu, Y. Komohara, Y. Fujiwara, H. Hirose, S. Futaki and T. Niidome, *ACS Omega*, 2020, **5**, 32744–32752.
58 T. S. Hauck, A. A. Ghazani and W. C. Chan, *Small*, 2008, **4**, 153–159.
59 L. Bao, X. Cai, M. Zhang, Y. Xiao, J. Jin, T. Qin and Y. Li, *J. Funct. Foods*, 2022, **90**, 104981.
60 S. S. Mathew-Steiner, S. Roy and C. K. Sen, *Bioengineering*, 2021, **8**, 63.
61 Y. Wang, Y. Feng, J. Yan, X. Han, P. Song, Y. Wu, X. Wang, Z. Mu, X. Li and H. Zhang, *Mater. Today Nano*, 2023, **23**, 100351.
62 B. Z. Johnson, A. W. Stevenson, C. M. Prêle, M. W. Fear and F. M. Wood, *Biomedicines*, 2020, **8**, 101.
63 T. Xiao, Z. Yan, S. Xiao and Y. Xia, *Stem Cell Res. Ther.*, 2020, **11**, 232.
64 P. Bao, A. Kodra, M. Tomic-Canic, M. S. Golinko, H. P. E hrlich and H. Brem, *J. Surg. Res.*, 2009, **153**, 347–358.
65 F. Shams, H. Moravvej, S. Hosseinzadeh, E. Mostafavi, H. Bayat, B. Kazemi, M. Bandehpour, E. Rostami, A. Rahimpour and H. Moosavian, *Sci. Rep.*, 2022, **12**, 18529.
66 H. G. Cha, J. Hur, C. J. Pak, J. P. Hong and H. P. Suh, *Int. Wound J.*, 2024, **21**, e14335.
67 S. S. Kuppa, J. Y. Kang, J. Y. Kim, G. Sa, J. H. Park, J. H. Kim, T. S. Ha, J. K. Seon, H. K. Kim and J. B. Lee, *Lasers Med. Sci.*, 2025, **40**, 171.
68 H. Lee, Y.-H. An, T. K. Kim, J. Ryu, G. K. Park, M. J. Park, J. Ko, H. Kim, H. S. Choi, N. S. Hwang and T. H. Park, *Adv. Biology*, 2021, **5**, 2000176.
69 G. T. Stavri, I. C. Zachary, P. A. Baskerville, J. F. Martin and J. D. Erusalimsky, *Circulation*, 1995, **92**, 11–14.
70 S. Dierckx, M. Patrizi, M. Merino, S. González, J. L. Mullor and R. Nergiz-Unal, *Front. Med.*, 2024, **11**, 1397517.
71 F. F. Felician, R. H. Yu, M. Z. Li, C. J. Li, H. Q. Chen, Y. Jiang, T. Tang, W. Y. Qi and H. M. Xu, *Chin. J. Traumatol.*, 2019, **22**, 12–20.
72 K. Kusnadi, H. Yedi, R. Emma, P. O. Nama, M. G. Amirah and M. Muchtaridi, *Int. J. Nanomedicine*, 2024, **19**, 11321–11341.
73 W. Liu, G. Zhang, J. Wu, Y. Zhang, H. Luo and L. Shao, *J. Nanobiotech.*, 2020, **18**, 9.